



EUROPEAN ORGANIZATION FOR NUCLEAR RESEARCH

CERN-EP/88-56
May 9th, 1988

SHADOWING IN DEEP INELASTIC MUON SCATTERING
FROM NUCLEAR TARGETS

The European Muon Collaboration

Aachen¹, CERN², DESY (Hamburg)³, Freiburg⁴, Hamburg (University)⁵,
Kiel⁶, LAL (Orsay)⁷, Lancaster⁸, LAPP (Annecy)⁹, Liverpool¹⁰, Marseille¹¹,
Mons¹², MPI (München)¹³, Oxford¹⁴, RAL (Chilton)¹⁵, Sheffield¹⁶,
Torino¹⁷, Uppsala¹⁸, Warsaw¹⁹, Wuppertal²⁰.

M. Arneodo¹⁷, A. Arvidson¹⁸, J.J. Aubert¹¹, B. Badelek^{19a}),
J. Beaufays², C.P. Bee^{8b}), C. Benchouk¹¹, G. Berghoff¹, I. Bird^{8c}),
D. Blum⁷, E. Böhm⁶, X. de Bouard⁹, F.W. Brasse³, H. Braun²⁰, C. Broll⁹⁺),
S. Brown^{10d}), H. Brück^{20e}), A. Brüll³, H. Calen¹⁸, J.S. Chima^{15f}),
J. Ciborowski^{19a}), R. Clifft¹⁵, G. Coignet⁹, F. Combley¹⁶, J. Coughlan^{8g}),
G. D'Agostini¹¹, S. Dahlgren¹⁸, F. Dengler¹³, I. Derado¹³, T. Dreyer⁴,
J. Drees²⁰, M. Drobnitzki¹, M. Düren¹, V. Eckardt¹³, A. Edwards^{20h}),
M. Edwards¹⁵, T. Ernst⁴, G. Eszes⁹ⁱ), J. Favier⁹, M.I. Ferrero¹⁷,
J. Figiel^{5j}), W. Flauger³, J. Foster^{16k}), J. Ftacnik¹³, E. Gabathuler¹⁰,
J. Gajewski⁵, R. Gamet¹⁰, J. Gayler³, N. Geddes^{14g}), P. Grafström^{18l}),
L. Gustafsson^{18q}), J. Haas⁴, E. Hagberg¹⁸, F.J. Hasert^{1m}), P. Hayman¹⁰,
P. Heusse⁷, M. Jaffré⁷, A. Jacholkowska²ⁿ), F. Janata⁵, G. Jancso¹³ⁱ),
A.S. Johnson^{14o}), E.M. Kabuss⁴, R. Kaiser⁴, G. Kellner², V. Korbel³,
A. Krüger⁵, J. Krüger^{20e}), S. Kullander¹⁸, U. Landgraf⁴, D. Lanske¹,
J. Loken¹⁴, K. Long^{14g}), M. Maire⁹, P. Malecki¹³, A. Manz¹³,
S. Maselli^{17p}), W. Mohr⁴, F. Montanet¹¹, H.E. Montgomery^{2q}), E. Nagy⁹ⁱ),
J. Nassalski^{19r}), P.R. Norton¹⁵, F.G. Oakham^{15s}), A.M. Osborne²,
C. Pascaud⁷, B. Pawlik¹³, P. Payre¹¹, C. Peroni¹⁷, H. Peschel²⁰,
H. Pessard⁹, J. Pettingale¹⁰, B. Pietrzyk¹¹, U. Pietrzyk^{20t}),
B. Pönsgen^{5u}), M. Pötsch^{20v}), P. Renton¹⁴, P. Ribarics⁹ⁱ), K. Rith^{4c}),
E. Rondio^{19a}), A. Sandacz^{19r}), M. Scheer¹, A. Schlagböhmer⁴,
H. Schiemann⁵, N. Schmitz¹³, M. Schneegans⁹, M. Scholz¹, T. Schröder⁴,
K. Schultze¹, A. Seidel⁴, T. Sloan⁸, H.E. Stier⁴, M. Studt⁵,
G.N. Taylor^{14w}), J.M. Thénard⁹, J.C. Thompson¹⁵, A. de la Torre^{5x}),
J. Toth⁹ⁱ), L. Urban¹, L. Urban⁹ⁱ), W. Wallucks⁴, M. Whalley^{16y}),
S. Wheeler¹⁶, W.S.C. Williams¹⁴, S.J. Wimpenny^{10z}),
R. Windmolders¹², G. Wolf¹³, K. Ziemons¹

(Submitted to Physics Letters)

ABSTRACT

Results are presented on the ratio of the inelastic muon-nucleus cross section per nucleon for carbon and calcium relative to that for deuterium. The measurements were made in the kinematic range of low x (0.003 - 0.1) and low Q^2 (0.3-3.2 GeV²) at an incident muon energy of 280 GeV. The calcium to deuterium ratio shows a significant x dependence which is interpreted as a shadowing effect. No strong Q^2 dependence is observed. This suggests that the effect is due at least partially to parton interactions within the nucleus.

Addresses

- 1) III. Physikalisches Inst. A, Physikzentrum, Aachen, Germany.
 - 2) CERN, Geneva, Switzerland.
 - 3) DESY, Hamburg, Germany.
 - 4) Fakultät für Physik, Universität Freiburg, Germany.
 - 5) II Institut für Experimentalphysik, Universität Hamburg, Germany.
 - 6) II Institut für Kernphysik, Universität Kiel, Germany.
 - 7) Laboratoire de l'Accélérateur Linéaire, Université de Paris-Sud, Orsay, France.
 - 8) Department of Physics, University of Lancaster, U.K.
 - 9) Laboratoire d'Annecy de Physique des Particules, IN2P3, Annecy-le-Vieux, France.
 - 10) Department of Physics, University of Liverpool, U.K.
 - 11) Centre de Physique des Particules, Faculté des Sciences de Luminy, Marseille, France.
 - 12) Faculté des Sciences, Université de L'Etat à Mons, Belgium.
 - 13) Max-Planck-Institut für Physik und Astrophysik, München, Germany.
 - 14) Nuclear Physics Laboratory, University of Oxford, U.K.
 - 15) Rutherford and Appleton Laboratory, Chilton, Didcot, U.K.
 - 16) Department of Physics, University of Sheffield, U.K.
 - 17) Istituto di Fisica, Università di Torino, Italy.
 - 18) Department of Radiation Science, University of Uppsala, Sweden.
 - 19) Physics Institute, University of Warsaw, and Institute for Nuclear Studies, Warsaw, Poland.
 - 20) Fachbereich Physik, Universität Wuppertal, Germany.
-
- a) University of Warsaw, Poland.
 - b) Now at University of Liverpool, U.K.
 - c) Now at MPI für Kernphysik, Heidelberg, Germany.
 - d) Now at TESA S.A., Renens, Switzerland.
 - e) Now at DESY, Hamburg, W. Germany.
 - f) Now at British Telecom, PLC, Ipswich, U.K.
 - g) Now at RAL, Chilton, Didcot, U.K.
 - h) Now at Jet, Joint Undertaking, Abingdon, U.K.
 - i) Permanent address: Central Research Institute for Physics of the Hungarian Academy of Science, Budapest, Hungary.
 - j) Now at Institute of Nuclear Physics, Krakow, Poland.
 - k) Now at University of Manchester, U.K.
 - l) Now at CERN, Geneva, Switzerland.
 - m) Now at Krupp Atlas Elektronik GmbH, Bremen, Germany.
 - n) Now at Laboratoire de l'Accélérateur Linéaire, Université de Paris-Sud, Orsay, France.
 - o) Now at SLAC, Stanford, California.
 - p) Now at MPI, Munich, Germany.
 - q) Now at FNAL, Batavia, Illinois, U.S.A.
 - r) Institute for Nuclear Studies, Warsaw, Poland.
 - s) Now at NRC, Ottawa, Canada.
 - t) Now at MPI für Neurologische Forschung, Köln, Germany.
 - u) Now at Software AG, Darmstadt, Germany.
 - v) Now at LeCroy Research Systems GmbH, Heidelberg, Germany.
 - w) Now at University of Melbourne, Parkville, Australia.
 - x) Now at Universidad Nacional, Mar del Plata, Argentina.
 - y) Now at University of Durham, U.K.
 - z) Now at University of California, Riverside, U.S.A.
 - +) Deceased.

It is well known that the cross section (per nucleon) for interactions between real photons and nuclei gets smaller with increasing nucleon number A . The effect, called shadowing, is more pronounced at high photon energy as is evidenced by measurements of the ratio of the copper to the free-nucleon cross sections at photon energies between 20 and 185 GeV [1]. The ratio drops from a value of about 0.73 at 20 GeV to 0.65 at 132 GeV. A similar but smaller shadowing effect has been observed for virtual photons [2] in charged lepton production below 20 GeV and at low values of Q^2 , the negative of the squared four-momentum transferred from the incident lepton to the target and the mass of the virtual photon. In a previous high-energy experiment, muons of 209 GeV were used and there were indications of quite large shadowing effects over the whole range of Q^2 from 0.03 to 30 GeV² [3].

One explanation of shadowing is that the photon can be viewed as a superposition of virtual hadrons, the so-called vector dominance model, and a point-like component [4]. For high enough photon energies, these hadrons may live long enough to traverse a whole nucleus. Since hadrons are absorbed strongly in a nuclear medium, nucleons inside a nucleus are shadowed by the nucleons in the front surface. For the case of virtual photons no significant shadowing is expected for Q^2 values above one GeV² where the contribution to the cross section of the hadronic component is negligible compared with that of the point like one.

An alternative explanation of shadowing is offered by parton models in which a target nucleon is considered in the infinite momentum frame [5]. In this frame a parton carries a fraction of the momentum $x = Q^2/(2m\nu)$ where m is the nucleon mass and ν is the energy lost by the lepton in the lab system [5]. Shadowing arises because, at small x , partons from different nucleons overlap in space and interact, leading to a redistribution of parton momenta. One of the models [6] predicts shadowing at small values of x with antishadowing in the region of $x \sim 0.1$. The effects are independent of Q^2 as expected for partons. More recent computations, based on a QCD inspired model [7], lead to an x -dependent shadowing disappearing very slowly with increasing Q^2 .

In an attempt to clarify the situation and to analyse more accurately the region of small x and low Q^2 , we have measured deep inelastic scattering of positive muons of energy 280 GeV in the range $0.003 < x < 0.1$, $0.3 < Q^2 < 3.2$ GeV², $10 < \nu < 150$ GeV. The targets investigated were D₂, C and Ca and the target thicknesses were 16, 37 and 24 g/cm² respectively.

The experiment was performed in the CERN muon beam using the EMC setup, details of which have been published elsewhere [8]. In figure 1, a side view is shown of the components of the apparatus most relevant for the study of shadowing. There were about 10^7 muons per 1.5 s long pulse which was repeated every 10 s. The beam size at the target was about 6×4 cm² and the divergence less than 1 mrad.

The momentum of the incident muon was measured to an accuracy of 0.3% by a spectrometer in the beam line and the muon was located to an accuracy of 1 mm in position and 0.2 mrad in divergence by the scintillator hodoscopes BHA-A' and BHB-B'. The 1 m long liquid D₂ target was placed inside the first of the two magnets, the VSM, and the C and Ca targets were placed 1 m upstream of the D₂ target. The momenta of scattered particles were measured by means of the two magnets, the VSM and the FSM, which bent the particles in opposite directions in the horizontal plane so that there was practically no momentum dispersion at the hodoscopes BHC-D. The coordinates of the tracks were measured using 4 sets of multiwire proportional chambers (MWPC). The chambers POC with 8 planes and POA and POB with 6 planes each had a wire spacing of 1 mm while the chambers P45 with 8 planes had a spacing of 2 mm. Hadrons were stopped in a 2 m thick iron absorber with a hole, 15 × 15 cm², to let the beam pass through.

A special trigger processor [9], conceived as a pilot project of FASTBUS, was used to select muons scattered at angles down to 2 mrad, i.e. within the beam. The trigger was formed by using the hit patterns of the incident muon in 320 scintillator elements of 8 hodoscope planes (BHA-A', BHB-B') and, of the scattered muon in 211 elements in 4 planes (BHC, BHD, BHE, BHF). Only vertically and horizontally aligned elements were used to form the trigger decision. The FASTBUS processor was used to decide if the downstream muon was not colinear with the incident beam

muon. On receipt of a signal that a non-colinear muon had been detected the wire chambers of the spectrometer were read out. These events were then reconstructed off-line using the standard EMC software programs.

The cross section was extracted for each target using a Monte Carlo simulation of the experiment in which acceptance, measurement errors and efficiencies in the apparatus and in the event analysis were taken into account. It was necessary to compute the cross section for each target separately since the two solid (C, Ca) and the liquid deuterium targets were placed at different positions along the beam and data were acquired at different times. The radiative corrections, computed using the method of Mo and Tsai [10], are everywhere less than 35%.

The data are presented as ratios of cross sections and of structure functions, F_2 on carbon and calcium to those on deuterium. Cross section and structure function ratios are identical assuming that R , the ratio of the longitudinal to transverse photon cross sections, is independent of the target. Cross sections obtained from deuterium and carbon in three separate experimental runs showed agreement in the shape of the variation with x and Q^2 but differed by up to 5% in normalisation. Such normalisation differences could be ascribed to variations in efficiency of the first level of the FASTBUS processor which defined an incoming beam muon. These differences imply an overall normalisation uncertainty of 7% on the ratios presented here.

Figure 2 and table 1 show the measured cross section ratios for carbon and calcium targets to those for deuterium as functions of x for two Q^2 intervals. The ratios for calcium exhibit a significant shadowing at small x which is independent of Q^2 within errors. The indicated error bars are statistical only, while the solid lines show systematic errors other than those due to the normalisation uncertainty. The major contributions to the systematic errors of the ratios of the cross sections are typically: 6% for acceptance correction, 3% for trigger inefficiency, 1.5% for losses in the selection of events from raw data, 1.5% for radiative corrections and 1.2% for errors in the momentum measurement of the incident and scattered muons. For each error source, the difference between the nominal and the distorted ratios was taken as the error and the different errors were added quadratically.

The ratios of cross sections shown in figure 2 rise with x similarly in the two selected Q^2 intervals and rise more strongly for Ca/D than for C/D. The lack of a Q^2 dependence suggests that vector meson dominance is not the main source of shadowing seen in our data. In this context it is interesting to note that indications of shadowing have been observed in the comparison of ν Ne and ν D data [11]. These indications are found to be limited to low Q^2 but rather independent of x .

Figure 3 shows the x dependence of our data and of data from other high-energy charged lepton scattering experiments [3,12,13,14,15]. The bars represent statistical and

systematic errors combined in quadrature wherever the latter ones are available. Our data extrapolate smoothly to those obtained with real photons ($Q^2 = 0$) of 60 GeV [1] and join to those obtained with electrons and muons at larger x . The x values of the points obtained in the Fermilab experiment at 209 GeV [3] were computed by dividing the published Q^2 values by $2m\nu$ using $\nu = 150$ GeV, an average value for their acceptance region ($110 < \nu < 200$ GeV for $Q^2 < 3$ GeV² and $40 < \nu < 200$ GeV for $Q^2 > 3$ GeV²).

Together the data give a clear evidence of an x -dependent shadowing which does not seem to depend on Q^2 . The data are also consistent with some antishadowing for x between 0.1 and 0.3. It is interesting to note that according to the model used in ref. [6] both shadowing and antishadowing should occur. Antishadowing should become negligible for $x > 0.15$ and the crossover x_c between shadowing and antishadowing is predicted to vary with A roughly as $x_c = 0.15 A^{-1/3}$. This prediction is not confirmed by the data of figure 3. However, the data are in qualitative agreement with the QCD inspired model [7] which predicts no antishadowing and a weak increase with A of the x value separating shadowing and no shadowing, once surface effects in the nucleus are included [16]. In this model, the shadowing effect arises because at small x , gluons from different nucleons annihilate which leads to a smaller number of gluons per nucleon in a nucleus than in a "free" nucleon. The number of quark-antiquark pairs, which are

created by the gluons, dominate the structure function at low x and will be reduced correspondingly.

In summary we have observed a significant shadowing signal in the x dependence of cross section ratios. This signal is almost insensitive to Q^2 i.e. it scales which suggests that parton interactions contribute to the shadowing.

We wish to thank many people at our home institutes and at CERN for support to this experiment. In particular, we thank A. Davies, R. Dobinson and E. Watson for their help with the small angle trigger. In addition, we thank the SPS division for providing us with the muons and, the DD and EP divisions for helping us with the FASTBUS pilot project. Finally the financial support from agencies in home countries and from CERN is gratefully acknowledged.

References

- [1] D.O. Caldwell et al., Phys. Rev. Lett. 42 (1979) 553 and references therein.
- [2] For a compilation of low energy leptonproduction data see for instance:
J. Franz et al., Z. Phys. C10 (1981) 105.
- [3] M.S. Goodman et al., Phys. Rev. Lett. 47 (1981) 293.
- [4] G. Grammer and J. Sullivan, in "Electromagnetic Interactions of Hadrons", edited by A. Donnachie and G. Shaw, Plenum Press (1978).
- [5] J.D. Bjorken, Phys. Rev. 179 (1969) 1547.
- [6] N.N. Nikolaev and V.I. Zakharov, Phys. Lett. 55B (1975) 397.
- [7] A.H. Müller and J. Qiu, Nucl. Phys. B268 (1986) 427.
J. Qiu, Nucl. Phys. B291 (1987) 746.
- [8] EMC, O.C. Allkofer et al., Nucl. Inst. and Meth. 179 (1981) 445;
EMC, J.P. Albanese et al., Nucl. Inst. and Meth. 212 (1983) 111.
- [9] A. Arvidsson et al., Nucl. Inst. and Meth. A251 (1986) 437.
- [10] L.W. Mo and Y.S. Tsai, Rev. Mod. Phys. 41 (1969) 205.
- [11] J. Guy et al., Z. Phys. C3 (1987) 337.
- [12] EMC, J. Ashman et al., CERN-EP-88/06, submitted to Phys. Lett.
- [13] SLAC, S. Stein et al., Phys. Rev. D12 (1975) 1884.
- [14] BCDMS, G. Bari et al., Phys. Lett. 163B (1985) 282.

- [15] BCDMS, A.C. Benvenuti et al., Phys. Lett. 189B
(1987) 483.
- [16] E.L. Berger and J. Qiu, Preprint ANL-PR-88.

Figure Captions

- Fig. 1 Side view of the EMC setup with components of main interest for the shadowing experiment. VSM and FSM denote the two magnets with a bending power of 5.2 Tm each. S_i are scintillators defining the beam. BHA and BHB contain 6 hodoscope planes each having 60 scintillator strips and BHA' and BHB' 4 planes each having 20 strips. POA-C and P45 are MWPC's. BHC consists of 144 scintillator bits ($1.4 \times 1.4 \text{ cm}^2$) arranged in a 12×12 matrix. BHD-F are single hodoscope planes having 1.5 cm wide strips.
- Fig. 2 Cross-section ratios versus x obtained for two different intervals of Q^2 : $0.3 < Q^2 < 1.0 \text{ GeV}^2$ (left side) and $1.0 < Q^2 < 3.2 \text{ GeV}^2$ (right side). The bars give the statistical errors and the solid lines enclosing the data points are limits within which the systematic errors may vary. In addition there is an error of 7% due to the uncertainty in normalisation.
- Fig. 3 Structure function ratios obtained in this experiment for the range $0.3 < Q^2 < 3.2 \text{ GeV}^2$ compared with other leptonproduction experiments: Ashman [12], Bari [14], Benvenuti [15], Goodman [3]. The points on the vertical axis are ratios from a photoproduction experiment, Caldwell [1], where the energy of the photon beam was 60 GeV. Error bars represent summed statistical and systematical errors. The arrows,

labelled x_C , define the transition point between shadowing and antishadowing according to ref. [6].

Table 1. Ratios with errors of the carbon and calcium cross sections relative to those of deuterium for the ν range 10-150 GeV. The errors are in percentages.

Q^2 range	$\langle Q^2 \rangle$	x	$\sigma(C)/\sigma(D)$	Stat. error	Syst. error
$Q^2 = .3-1$.52	.0035	.86	.06	.05
	.60	.0050	.87	.04	.04
	.61	.0075	.91	.05	.05
	.61	.0105	.90	.05	.04
	.63	.015	.89	.04	.04
	.68	.024	.92	.05	.04
	.90	.04	.92	.06	.05
	$Q^2 = 1.-3.2$	1.09	.0050	.93	.12
1.25		.0075	.93	.07	.05
1.54		.0105	.98	.07	.05
1.74		.015	.95	.05	.04
1.76		.024	.91	.04	.04
1.68		.04	.92	.04	.05
1.71		.06	1.02	.04	.05
2.29		.09	1.03	.05	.05
Q^2 range	$\langle Q^2 \rangle$	x	$\sigma(Ca)/\sigma(D)$	Stat. error	Syst. error
$Q^2 = .3-1$.52	.0035	.71	.04	.06
	.60	.0050	.78	.03	.06
	.61	.00075	.81	.03	.06
	.61	.0105	.83	.04	.06
	.63	.015	.83	.03	.05
	.68	.024	.88	.04	.04
	.90	.04	.95	.05	.05
	$Q^2 = 1.-3.2$	1.09	.0050	.76	.08
1.25		.0075	.79	.05	.04
1.54		.0105	.82	.05	.04
1.74		.015	.84	.04	.04
1.76		.024	.90	.03	.04
1.68		.04	.96	.03	.05
1.71		.06	1.08	.04	.05
2.29		.09	.98	.04	.05

Table 1 cont'd

x range	$\langle x \rangle$	Q^2	$\sigma(c)/(D)$	Stat. error	Syst. error
x = .004- .018	.009	.35	.94	.06	.04
	.011	.50	.88	.04	.04
	.010	.70	.91	.04	.05
	.010	.90	.89	.05	.04
	.010	1.10	.97	.06	.05
	.011	1.40	.98	.06	.05
	.013	2.00	.93	.06	.05
	.015	2.80	.85	.10	.04
x = .018- .11	.033	.5	.92	.06	.05
	.028	.7	.97	.06	.05
	.040	.9	.89	.04	.04
	.050	1.1	.98	.05	.05
	.051	1.4	.98	.04	.05
	.061	2.0	1.01	.04	.04
	.058	2.8	.87	.04	.03
	.056	3.6	.90	.06	.04
	.055	4.4	.83	.07	.03
	.063	5.6	.80	.07	.03
x range	$\langle x \rangle$	Q^2	$\sigma(Ca)/\sigma(D)$	Stat. error	Syst. error
x = .004- .018	.009	.35	.85	.05	.07
	.011	.50	.85	.03	.08
	.010	.70	.82	.03	.07
	.010	.90	.76	.03	.05
	.010	1.10	.82	.04	.04
	.011	1.40	.87	.04	.04
	.013	2.00	.79	.04	.05
	.015	2.80	.74	.07	.07
x = .018- .11	.033	.5	.93	.05	.08
	.028	.7	.89	.05	.05
	.040	.9	.89	.04	.04
	.050	1.1	.93	.04	.04
	.051	1.4	1.03	.04	.04
	.061	2.0	.99	.03	.05
	.058	2.8	.92	.04	.07
	.056	3.6	.81	.04	.07
	.055	4.4	.93	.06	.11
	.063	5.6	.86	.06	.12

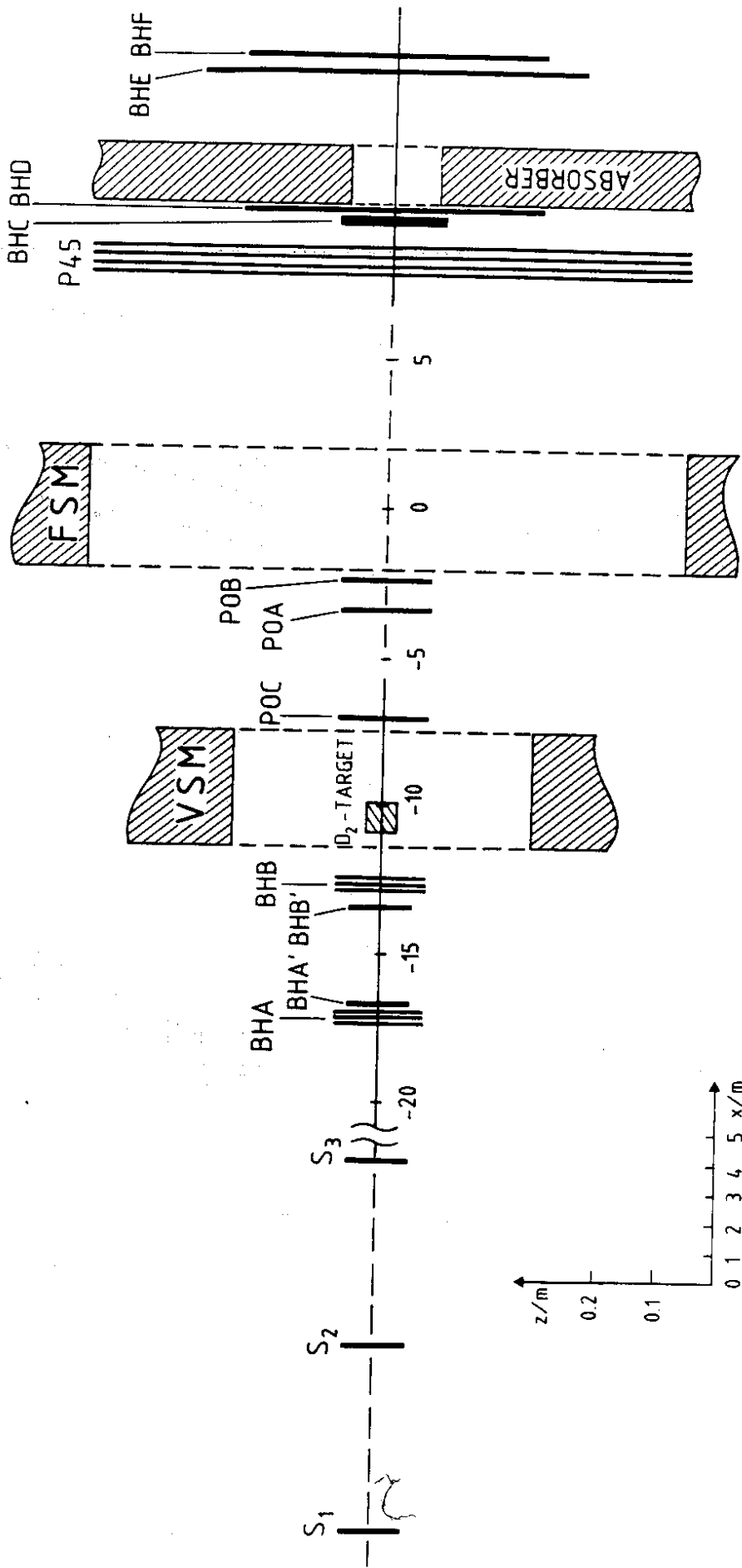


Fig. 1

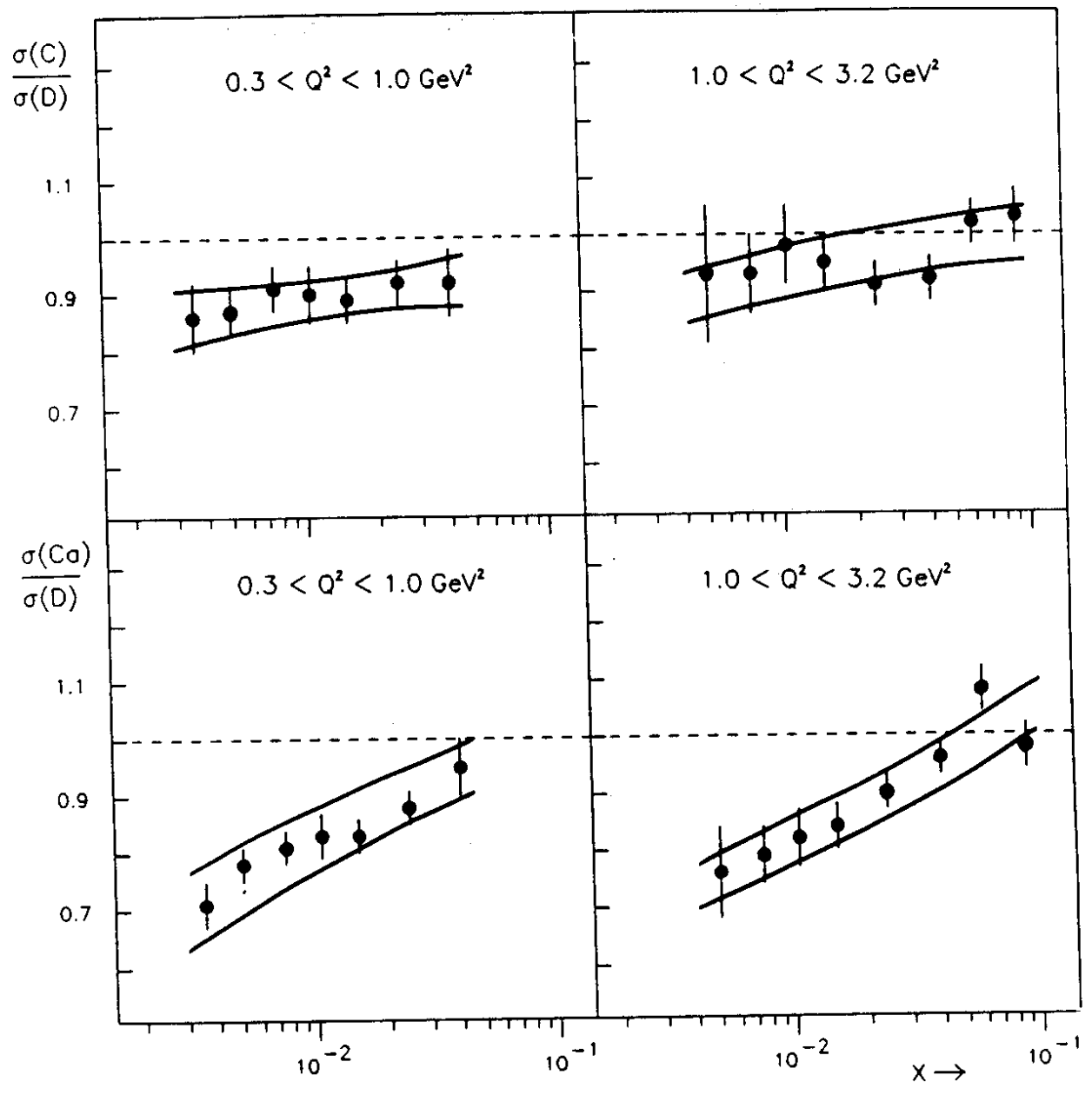


Fig. 2

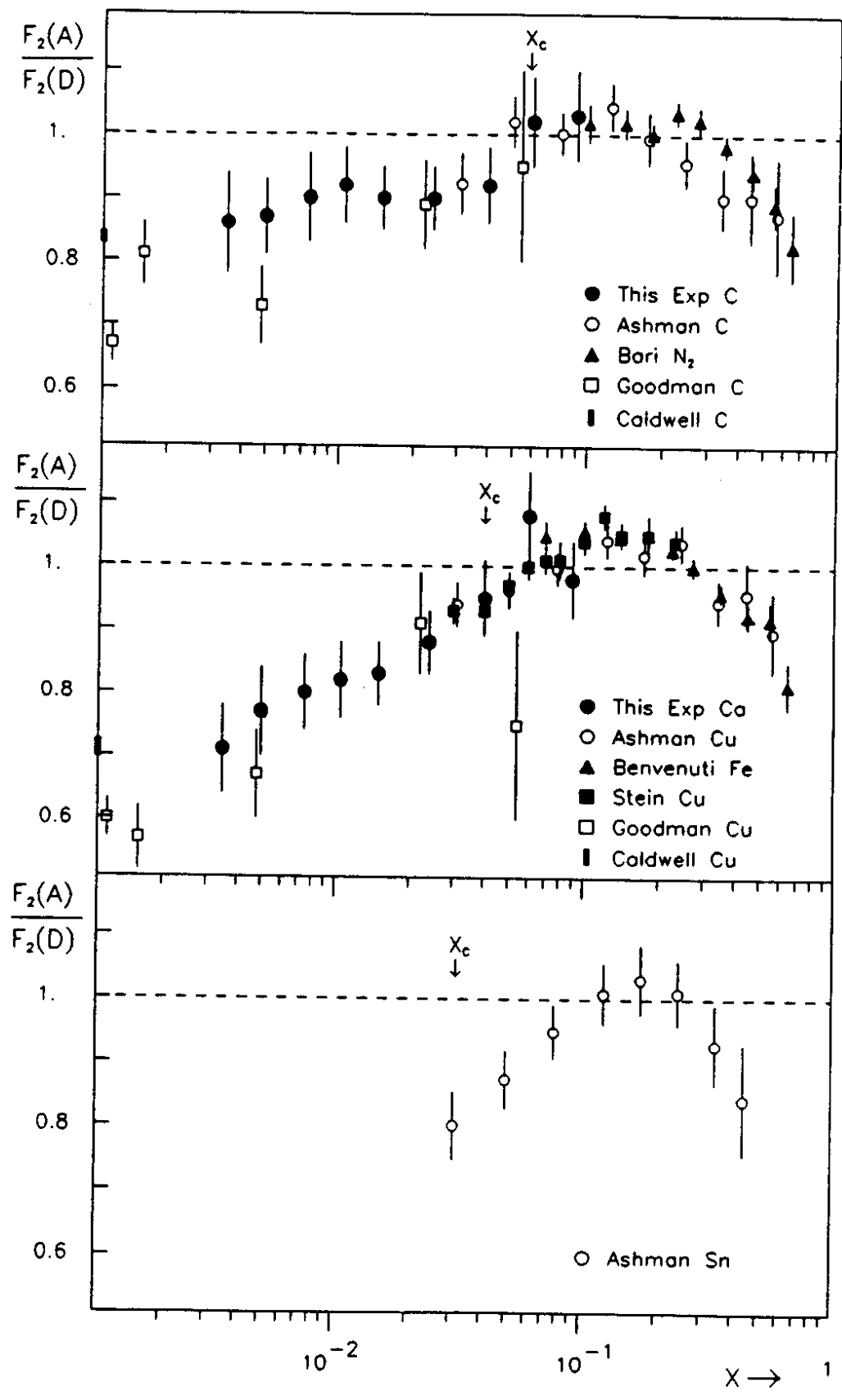


Fig. 3